Advances in Environmental Technology 4 (2022) 329-343

Iranian Reasearch Organization for Science and Technology (IROST)

Advances in Environmental Technology

Journal home page: https://aet.irost.ir/

Low-cost magnetic char derived from oily sludge for Methylene Blue dye removal: optimization, isotherm, and kinetic approach

Saeedeh Rastgar[1], Hassan Rezaei[1*], Habibollah Younesi[2*], Hajar Abyar[1*]

[1]Department of Environmental Sciences, Faculty of Fisheries and Environmental Sciences, Gorgan University of Agricultural Sciences and Natural Resources, Gorgan, Iran

[2]Department of Environmental Science, Faculty of Natural Resources, Tarbiat Modares University, Noor, Iran

ARTICLE INFO

Document Type:
Research Paper

Article history:
Received 13 August 2022
Received in revised form
30 October 2022
Accepted 1 November 2022

Keywords:
Oily sludge
Methylene Blue adsorption
Magnetic char
Kinetic modeling

ABSTRACT

The excessive increase of dye-contaminated wastewater has become an environmental challenge worldwide, menacing human beings, the environment, and the ecosystem. In light of this subject, the current study for the first time evaluated the potential of oily sludge with its intrinsic magnetic characteristics for Methylene Blue adsorption. A single-step pyrolysis approach was employed to convert oily sludge to magnetic char (Fe_3O_4/Char). The effects of operational parameters such as pH, contact time, Methylene Blue concentration, and adsorbent dose were examined. The maximum adsorption was 84% with a capacity of 88.71 mg/g at a pH of 3, 100 mg/L Methylene Blue concentration, 100 mg Fe_3O_4/Char concentration, and 120 min contact time. The Redlich-Peterson isotherm model (R^2= 0.9854) best described the adsorption experiment, which revealed that the adsorption process followed a mixed adsorption mechanism, namely physical and chemical adsorption. Moreover, the Elovich kinetic model was more suitable to represent the Methylene Blue adsorption onto Fe_3O_4/Char, confirming a chemisorption process. The significant function of the sludge-based char with high iron content in the adsorption of Methylene Blue provides insight into the inherent potential of oily sludge as a promising approach for removing hazardous dyes.

1. Introduction

Over the last decades, urbanization, industrialization, and rapidly changing technologies have intensified water and chemical utilization, resulting in water pollution. Various industries, such as textiles, pulp and paper, food processing, and cosmetics, produce dyed and toxic wastewater, threatening human health and the environment [1]. In this context, the textile industry is a significant source of dye wastewater due to the high demand for textile products and large volumes of water consumption. Notably, 1000 L of water is utilized for processing 1000 kg of clothes in the dying steps [2]. On the other hand, the textile industry uses 60-70% azo dyes, releasing 15-20% of

*Corresponding author:
E-mail: Hassanrezaei@gau.ac.ir, hunesi@modares.ac.ir, hajar.abyar@gau.ac.ir
DOI:10.22104/AET.2022.5795.1595

the total dye into water bodies [3]. The escalation of dye compounds in water resources leads to dissolved oxygen (DO) depletion, hindering sunlight penetration into the water surface and impairing the biological activity of aquatic organisms [4,5]. Photosynthesis reduction, a change in the aquatic environment, and dye bioaccumulation are other negative ecological consequences of dye deposition that deteriorate the water quality and introduce toxic chemicals into the food chain [6]. Generally, dyes are highly stable, toxic, hydrophobic, bio-accumulative, and resistant to photolysis, making them persistent in aquatic ecosystems [7]. Methylene Blue is a cationic dye often used to dye wool, nylon, and silk, resulting in allergies, skin irritations, mutations, and cancer [8,9]. Exposure to and inhaling Methylene Blue induces serious damage to the reproductive system, kidney function, brain, liver, and central nervous system, as well as increasing the effluent's chemical oxygen demand (COD) [10]. Regarding the dyes' resistance to conventional physicochemical degradation, 60–70% of azo dyes are poisonous and resistant to standard treatment techniques, resulting in long-term hazards [11]. Hence, to achieve clean and safe water in accordance with environmental legislation, the dye wastewater should be treated physically, chemically, or biologically. The conventional techniques for dye wastewater treatment include membrane methods, coagulation-flocculation, sedimentation, electrochemical treatment, aerobic and anaerobic degradation, and chemical oxidation technologies [12,13]. Among the aforementioned methods, adsorption is the most widely used technique to remove dye components due to relatively low costs, operational simplicity, easy performance, safe by-products, and high recovery potential. In this regard, chars as carbon-based materials are suitable adsorbents for organic compounds [1,14]. Chars with a specific surface area and good porosity are able to adsorb cationic and anionic dyes at high temperatures [15]. Since chars can be produced from available industrial or agricultural wastes, they are not only economically efficient but also beneficial for waste reduction [16]. The quality of chars depends on the precursor characteristics, carbon content, thermal stability, chemical composition, and surface functional groups [17,18]. However, the utilization of chars on a large scale is limited due to practical obstacles such as filtration, dispersion, turbidity, secondary contamination, and the high cost of regeneration [19]. Therefore, the amelioration of chars' magnetic properties through the synthesis of iron oxide nanoparticles can facilitate their separation from water solutions [20]. There are numerous investigations considering char production for dye removal. Suhaimi, et al. [14] studied the adsorption of Methylene Blue from aqueous solutions using char. Locally grown bamboo (*Gigantochloa* spp.) was used as feedstock for biochar production under various pyrolysis temperatures (400–800 °C). The adsorption data confirmed that pyrolysis temperature had a significant effect on the adsorptive performance, and biochar pyrolyzed at 500 °C showed a maximum adsorption capacity equal to 86.6 mg/g [14]. Moreover, Han, et al. [21] used the oily sludge activated by H_3PO_4 for char production. The synthesized char exhibited favorable hierarchical porous properties, capable of adsorbing Methylene Blue (322.89 mg/g). According to the literature [22], biochar obtained from the green marine seaweed *Ulva reticulata* showed a maximum removal potential for Remazol brilliant orange 3R (91.6%) at a pH of 2 and a biochar dose of 2 g/L. Another study [23] illustrated the adsorption capacity of 153.84 mg/g for Methylene Blue using pine needle biomass. Although the chars originating from wastes were potentially apprised, the capability of oily sludge, aggregated in diesel tanks in petrochemical refineries, for dye removal has been less investigated [23]. Regarding the high production of oily sludge due to industrial development, the focus on modern and advanced techniques for the diminution of waste and its harmful impacts is urgently required. To close the gap, the current study endeavors to determine the oily sludge capacity as a precursor for char synthesis and Methylene Blue adsorption. Therefore, the current study proceeded as follows: (1) char synthesis from oily sludge, (2) evaluation of char potential to adsorb Methylene Blue, (3) optimization of adsorption process considering contact time, pH, adsorbent dosage, and initial concentration of

Methylene Blue, and (4) isotherm and kinetic assessment. The obtained results from this pioneering study provide a framework for dye removal in industrial wastewater.

2. Materials and methods

2.1. Synthesis of magnetic char (Fe_3O_4/Char)

The sludge required for Fe_3O_4/Char preparation was obtained from the National Iranian Oil Products Distribution Company located in Golestan, Gorgan, Iran. The intrinsic characteristics of the utilized precursor and its iron-rich content made it an ideal material for removing pollutants (C= 50.66%, H= 3.77%, N= 0.86%, and S= 1.89%). Synthesis of Fe_3O_4/Char was carried out in a one-step carbonization process. The oily sludge was dried at 110 °C for 24 h, then crushed and dried again at 70 °C. After that, the oily sludge was ground and sieved to attain a particle size of 0.4-0.8 mm. Afterward, the pyrolysis experiments were performed in a stationary horizontal stainless steel tube furnace at 550 °C under argon gas for 2 h. Finally, the synthesized char was collected and stored in an airtight container.

2.2. Characterization of Fe_3O_4/Char

The elemental analysis (C, H, N, S, and O) was performed by an elemental analyzer (Flash EA 1112, USA). Field scanning electron microscopy analysis (FESEM, MIRA111, Czech) was employed to evaluate the appearance characteristics and determine the size and morphology of the synthesized particles. The crystal structure of the particles was assessed by an X-ray diffractometer (XRD, Philip X, parts, PW1730 Netherlands). Fourier-transform infrared spectroscopy (FTIR; Thermo Nicolet Avatar 370 FT-IR, USA) analysis was performed to investigate the surface functional groups of Fe_3O_4/Char [8,9].

2.3. Batch adsorption experiment

The adsorption process was conducted in a batch system of 1000 mL Erlenmeyer flasks, considering various parameters, including pH, Methylene Blue concentration, adsorbent dose, and contact time. The stock of Methylene Blue solution (1000 mg/L) was prepared by dissolving $C_6H_{18}C_1N_3S_2H_2O$ in deionized water, and then the working solution of different concentrations was obtained by dilution of the stock solution. The effect of pH on the adsorption process was studied by mixing 100 mg of the synthesized char with the Methylene Blue solution at a concentration of 100 mg/L. The pH range of 2–9 was adjusted using 1 M HCl and 1 M NaOH solution. The prepared mixture was agitated on a stirrer at 250 rpm at room temperature (25 °C) until equilibrium conditions occurred (120 min). To optimize the dye concentration in the adsorption process, the Methylene Blue solution with a concentration of 25, 50, 75, 100, 125, 150, 175, and 200 mg/L at the optimum pH of 3 and an adsorbent dose of 100 mg was considered. After determining the optimum pH and dye concentration, the effect of the adsorbent doses of 25, 50, 75, 100, 125, 150, 175, and 200 mg on the adsorption process was investigated. For this purpose, the Methylene Blue solution with a concentration of 100 mg/L at a pH of 3 and a contact time of 120 min was examined to optimize the adsorbent dose. Afterward, the impact of the contact time of 25, 50, 75, 100, 125, 150, 175, and 200 min was assessed in the Methylene Blue solution with a concentration of 100 mg/L, pH of 3, and 100 mg of adsorbent. Finally, the experiment was conducted under a pH of 3, a contact time of 120 min, a dye concentration of 100 mg/L, and an adsorbent dosage of 100 mg. Then, 5 mL was sampled at an interval of 25 min, and the Methylene Blue concentration was measured by a spectrophotometer (Unico USA's UV-Vis 4802 dual-beam) at a wavelength of 664 nm. Blank samples containing deionized water were used as a control. The percentage of dye adsorption in each step was calculated using the following formulas [24]:

$$\mathrm{A}(\%) = \frac{100(C_0 - C_e)}{C_0} \quad (1)$$

$$\mathrm{q} = \frac{(\mathrm{C_0} - \mathrm{C_e})\mathrm{v}}{\mathrm{M}} \quad (2)$$

where C_o and C_e are the initial and equilibrium concentrations of Methylene Blue (mg/L), respectively; q denotes the amount of adsorbed Methylene Blue (mg/g); and V and M are the volume of the solution (L) and adsorbent mass (g), respectively.

2.4. Isotherm modeling

The Langmuir, Freundlich, Redlich-Peterson, and Temkin isotherm models were used. The Langmuir isotherm model is expressed as follows [17]:

$$q_e = \frac{q_m b C_e}{1 + b C_e} \quad (3)$$

The following equation was used for a linear fitting of the Langmuir isotherm model to the experimental data, C_e/q_e versus C_e.

$$\frac{C_e}{q_e} = \frac{1}{q_m b} + \frac{1}{q_m} C_e \quad (4)$$

where q_e is the equilibrium adsorbent-phase concentration of the adsorbate (mg/g), C_e is the equilibrium aqueous-phase concentration of adsorbate (mg/L), and b is the constant related to the free adsorption energy and the reciprocal of the concentration at which half saturation of the adsorbent is reached. Moreover, q_m is the maximum adsorption capacity (mg/g).

The Freundlich adsorption isotherm is described based on the following equations [25]:

$$q_e = K_F C_e^{\frac{1}{n}} \quad (5)$$

$$\ln q_e = \ln K_F + \frac{1}{n} \ln C_e \quad (6)$$

where q_m represents the amount of adsorbed molecules to the adsorbent surface at any time (mg/g), C_e is the equilibrium concentration (mg/L), and n and K_F are the Freundlich constant and Freundlich exponent (mg/g $(L/mg)^{1/n}$), respectively.

The Redlich-Peterson (R-P) model, a hybrid of the Langmuir and Freundlich isotherm models, is explained as follows [16]:

$$q_e = \frac{A_R C_e}{1 + B_R C_e^{\gamma}} \quad (7)$$

A linear plot of $ln(A_R(C_e/q_e)-1)$ versus lnC_e is attained as follows:

$$\ln\left(A_R \frac{C_e}{q_e} - 1\right) = \gamma \ln C_e + \ln B_R \quad (8)$$

where A_R is the Redlich-Peterson adsorption capacity constant (L/g) determined *via* trial and error to obtain the maximum linear regression value of the isotherm graph, B_R is the R-P isotherm constant (L/mg), and γ is the exponent between 0 and 1. The Temkin isotherm model is explained based on the following equations [25]:

$$q_e = \frac{RT}{b_T} \ln A_T C_e \quad (9)$$

$$q_e = \frac{RT}{b_T} \ln A_T + \frac{RT}{b_T} \ln C_e \quad (10)$$

where b_T is the Temkin isotherm constant (J/mol), R shows the universal gas constant (8.314 J/mol. K), T is the temperature (K), and A_T denotes the Temkin isotherm equilibrium binding constant (L/g).

2.5. Adsorption kinetics

Pseudo-first-order kinetic model is expressed as follows [7]:

$$\frac{dq_t}{d_t} = k_1 (q_{e1} - q_t) \quad (11)$$

$$\ln(q_{e1} - q_t) = \ln q_{e1} - k_1 t \quad (12)$$

where q_{e1} and q_t represent the adsorbed amount of the adsorbate at equilibrium time and at time t (mg/g), respectively, and K_1 is the pseudo-first-order rate constant (1/min). The pseudo-second-order kinetic model is also described as follows [10]:

$$\frac{dq_t}{d_t} = k_1 (q_{e1} - q_t) \quad (13)$$

$$\frac{t}{q_t} = \frac{1}{k_2 q_{e2}^2} + \frac{1}{q_{e2}} t \quad (14)$$

where k_2 is the pseudo-second-order constant rate (g/mg. min) and t is the time (min). The Elovich model is expressed as follows [26].

$$\frac{dq_t}{dt} = \alpha e^{-\beta q_t} \quad (15)$$

The rate parameter for the Elovich equation is determined as:

$$q_t = \frac{1}{\beta} \ln(\alpha\beta) + \frac{1}{\beta} \ln t \quad (16)$$

where α represents the initial adsorption rate constant (mg/g min) and β is the Elovich constant associated with the extent of surface coverage and activation energy involved in chemisorption (g/mg).

3. Results and discussion

3.1. Characterization of Fe_3O_4/Char

The morphology of the Fe_3O_4/Char was determined by FESEM analysis (Figure 1), which demonstrated a relatively irregular structure with visible protrusions and pores. The existence of fine pores on the surface of the Fe_3O_4/Char was attributed to the release of volatile matters during pyrolysis [27].

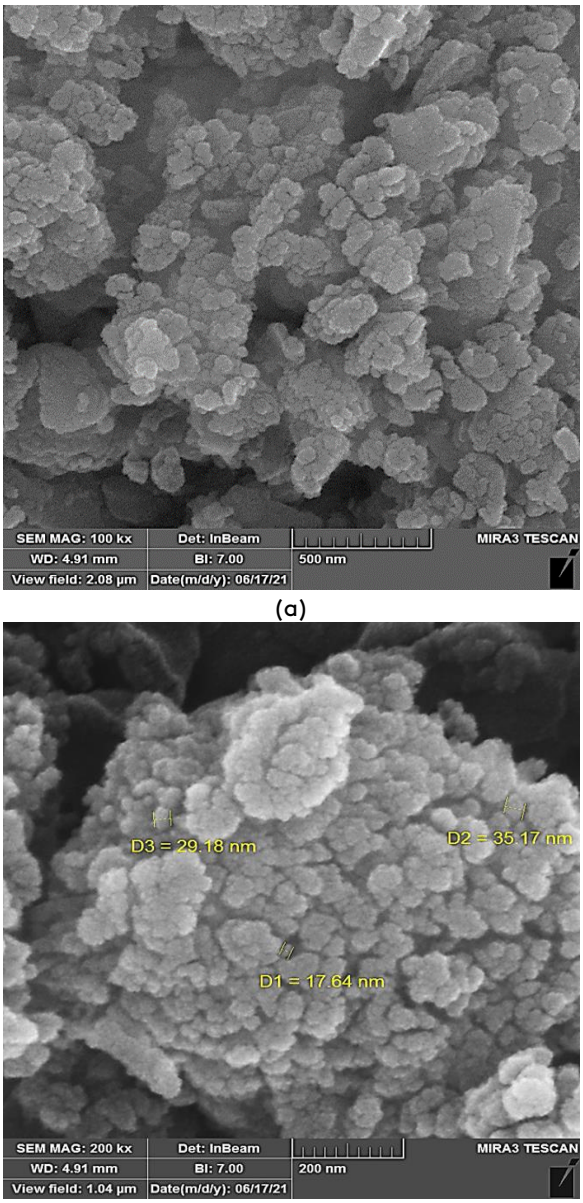

Fig. 1. FESEM images of the Fe_3O_4/Char, 100x (a) and 200x (b).

The crystal structure of the Fe_3O_4/Char was investigated using XRD, as illustrated in Figure 2. As can be seen in Figure 2, the content of carbon in the Fe_3O_4/Char was increased compared to the initial oily sludge, while some elements vanished in the Fe_3O_4/Char after the oxidation process. Based on the Fe_3O_4/Char diagram, clear and sharp peaks at 111, 222, and 002° could correspond to Fe_3O_4 particles, which were observable in the sludge diagram with lower intensity [14]. Moreover, the organic matter in the oily sludge was converted to the magnetic char under the pyrolysis process, which was confirmed by the presence of Fe_3O_4 peaks [28]. The surface chemistry of the synthesized Fe_3O_4/Char was evaluated using FTIR analysis. As shown in Figure 3, the FTIR spectrum was recorded in the adsorption band of 400-4000 cm^{-1}. The broad peak at 3467.15 cm^{-1} corresponded to O-H bonds of hydroxy organic compounds. The band at 1621.16 cm^{-1} was related to the presence of C=O stretching. The peak located at 1380.13 cm^{-1} could be ascribed to the CH_2 bonds [29]. Also, the peak at 1128.29 cm^{-1} was associated with the C-O bonds of the epoxy group, the evidence for oxygen-rich functional groups. The bands at 363.56 cm^{-1} and 470.26 cm^{-1} were due to Fe-O and Fe-OH stretching, respectively [30,31].

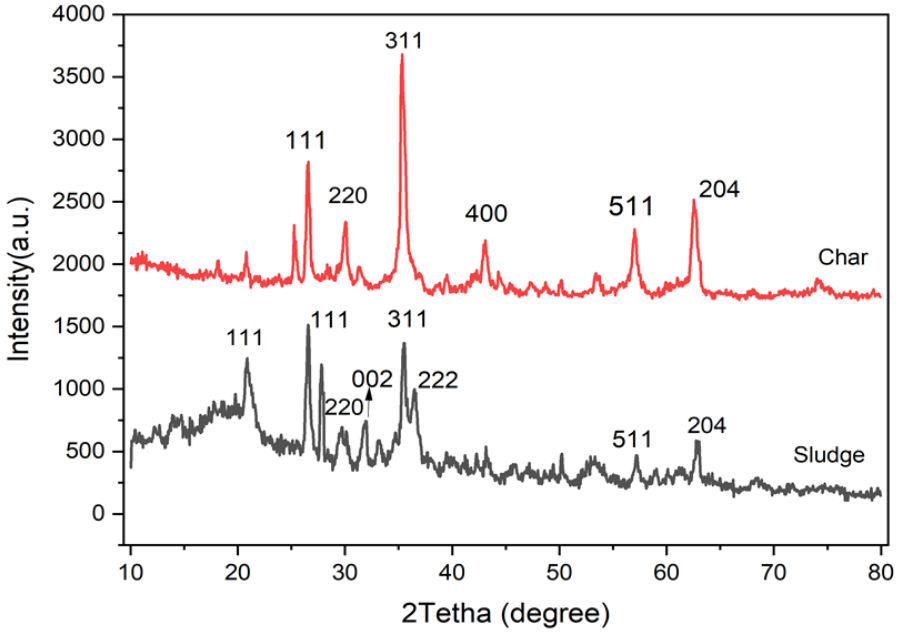

Fig. 2. XRD analysis of Fe_3O_4/Char.

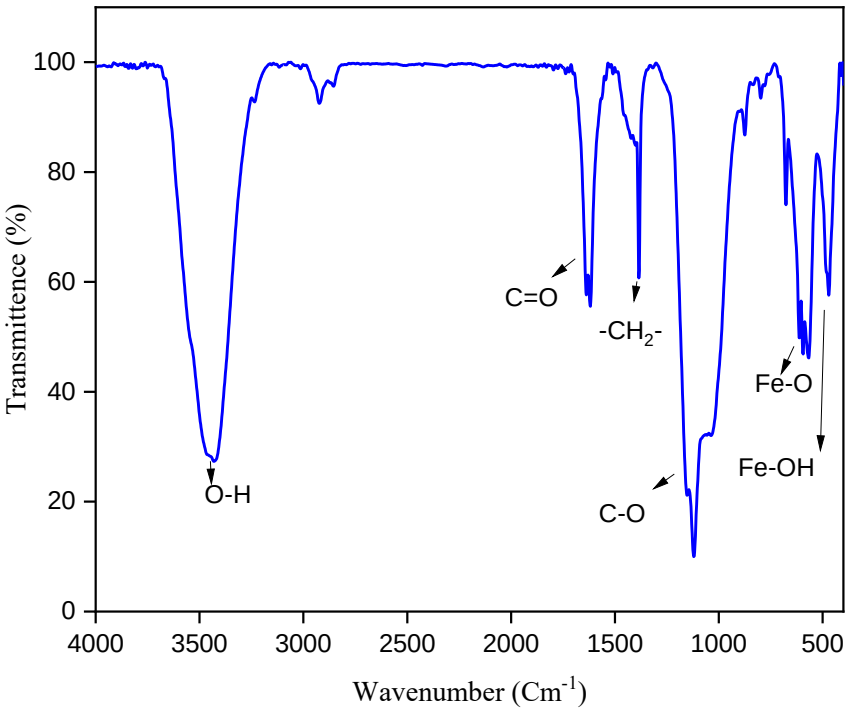

Fig. 3. FTIR spectrum of Fe_3O_4/Char.

3.2. Effect of pH

Figure 4a displays the impact of pH on the adsorption rate of Methylene Blue by the synthesized Fe_3O_4/Char. According to the results, the Methylene Blue adsorption decreased while the pH solution increased. The maximum and minimum adsorption percentages were detected at pH 3 and 9, equal to 96.82% and 43.47%, respectively. The decline in adsorption efficiency could be attributed to the electrostatic attraction between the adsorbent surface and the dye molecules due to the increase of OH^- ions [32]. In this regard, Hevira, et al. [4] used a cost-effective adsorbent derived from *Terminalia catappa* shells to remove Methylene Blue from the aqueous

solution and reported the highest adsorption at a pH of 5. In addition, Li, et al. [33] investigated the capability of four prepared lignins for Methylene Blue adsorption, in which the maximum adsorption was observed at pH 4. In contrast, Jabar, et al. [34] declared that the optimum pH for the Methylene Blue adsorption by *Terminalia catappa L* was eight because of the electrostatic repulsion between the cationic Methylene Blue and the surface of the biochar. Therefore, according to Figure 4a, the optimum adsorption capacity of Fe_3O_4/Char was at pH 3, indicating more available sites to bind with Methylene Blue molecules [34]. The adsorption capacity showed the same trend as Methylene Blue removal, which decreased from 110.13 mg/g to 49.44 mg/g with a pH increase in the range of 3-9. Notably, the adsorption capacity illustrated a lower alteration (~1%) in pH 2 and 3. This observation was consistent with Liu, et al. [35]; they declared that the removal of Methylene Blue reached the maximum (414.25 mg/g) at the pH of 2. In fact, the catalytic ability is upgraded in acidic conditions, and the pH increase leads to iron and oxyhydroxide precipitation in the solution [35]. Furthermore, Zhang, et al. [36] found a fast increase in adsorption capacity by the pH increasing to three, which confirmed the results of the present study. Generally, at a pH value of one, the competition between hydrogen ions and adsorption sites on the adsorbent surface decreases the Methylene Blue removal, whereas the electrostatic attraction between the positively charged surface of the adsorbent and negatively Methylene Blue molecules increases the adsorption capacity due to the decline in hydrogen ions. However, the negative charge of the adsorbent at higher pH limits the adsorption capacity [37].

3.3. Effect of adsorbent dose

As shown in Figure 4b, the adsorption process was appraised at an adsorbent dose of 25, 50, 75, 100, 125, 150, 175, and 200 mg. Regarding the obtained results, the increase of the adsorbent dose from 25 mg to 100 mg led to an adsorption enhancement from 30.73% to 93.17%, respectively, whereas a relatively decreasing trend was observed when the adsorbent dose was increased from 100 mg to 200 mg.

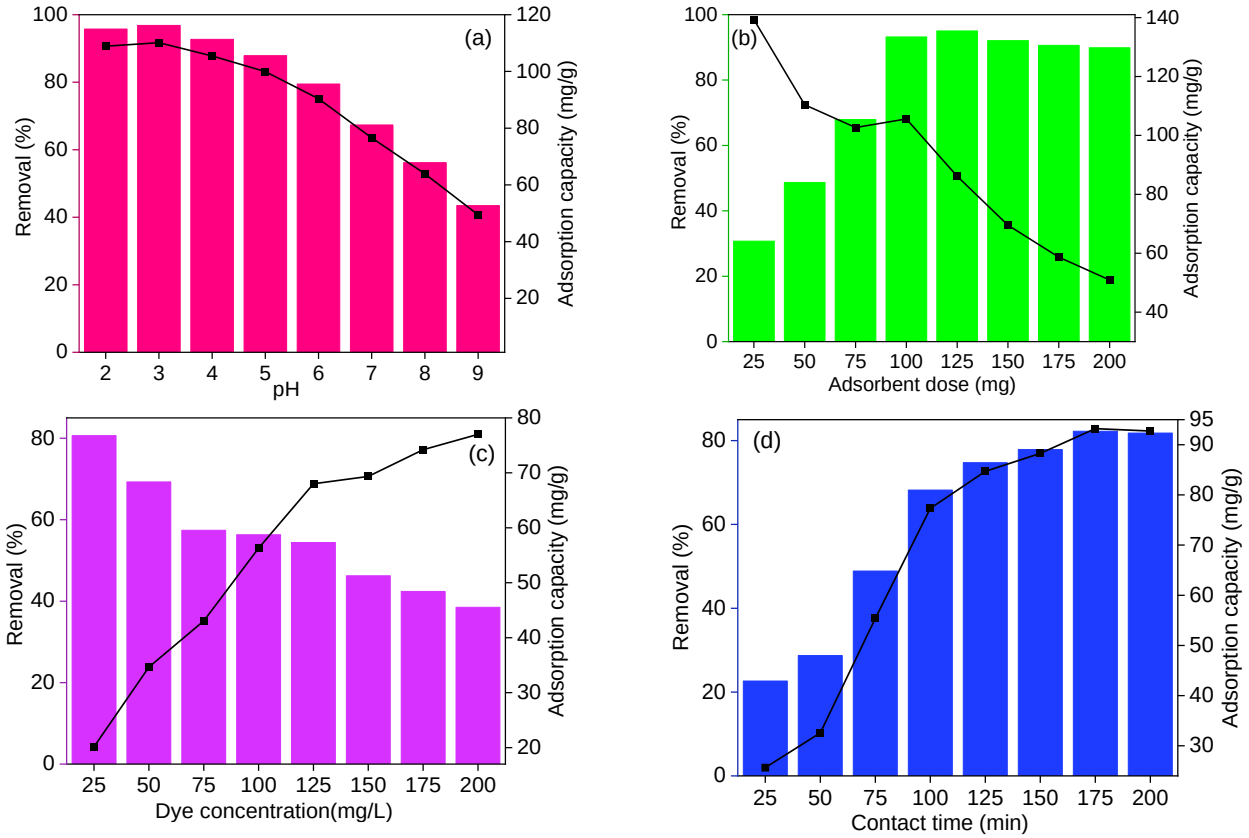

Fig. 4. Effects of operational variables on the Methylene Blue adsorption, pH (a), adsorbent dose (b), Methylene Blue concentration (c), and contact time (d).

Generally, the number of available active sites on the synthesized adsorbent increased at higher dosages, leading to more trapped Methylene Blue molecules [38]. Moreover, the increase of functional groups such as hydroxyl and superoxide radicals caused an increment in the adsorption percentage. However, if the adsorbent dose exceeds a certain limit, the suspended particles collide, and the active sites on the adsorbent are deactivated [39]. On the other hand, the accumulation of adsorbents and the interaction of particles reduce the effective surface of adsorbents. The obtained results were in agreement with Das and Goud [40], who utilized biochar derived from agricultural waste and reported almost 88.3% of ranitidine removal at pH 9 and 100 mg of adsorbent. Furthermore, Jabar and Odusote [8] assessed the potential of biochar originating from oil palm empty fruit bunch fiber to remove Cibacron Blue 3G-A dye from an aqueous solution. The optimum adsorbent dose was 0.10 g/100 mL, which confirmed the results of this study. The adsorption capacity revealed a decreasing trend from 139.33 mg/g to 50.94 mg/g, while the adsorbent dose was increased from 25 mg to 200 mg due to a lack of Methylene Blue in the solution [41]. Since the Methylene Blue molecules were adsorbed on the adsorbent surface because of an increase in the availability of active sites, adding more adsorbents did not affect the adsorption capacity and might leave empty adsorption sites [42]. In this regard, Kooh, et al. [43] reported a decline in the adsorption capacity of Azolla pinnata in the removal of Methylene Blue when the adsorbent dosage increased from 0.01 g to 0.08 g.

3.4. Effect of dye concentration

The impact of initial Methylene Blue concentration was evaluated at a fixed pH, adsorption dosage, and contact time. Figure 4c depicts that the amount of adsorption decreased in proportion to the increase in dye concentration. The highest adsorption (80.65%) was detected at a 25 mg/L Methylene Blue concentration, which dropped down to 38.5% at a concentration of 200 mg/L. Notably, the adsorption percentage showed a low alteration while the Methylene Blue concentration varied from 25 mg/L to 100 mg/L. Hence, the dye concentration of 100 mg/L was chosen as the optimum one. It should be mentioned that more adsorption sites are accessible at low dye concentrations, and Methylene Blue molecules could react with the existing adsorption sites on the surface of the adsorbent, increasing adsorption efficiency [44]. In contrast, the adsorption capacity was enhanced in proportion to the increment of dye concentration. It can be explained that the whole adsorbate molecules interacted with the active adsorption sites at low dye concentrations [19]. However, at high dye concentrations, each active adsorption site was surrounded by a more significant number of Methylene Blue molecules, leading to the increase in adsorption quantity per unit mass of the adsorbent [23]. These processes reduce the adsorption efficiency by increasing the initial dye concentration. The results were in accordance with Viswanthan, et al. [12]; they used biochar for the Methylene Blue adsorption in the range of 50-250 mg/L and reported the highest adsorption (90%) at a concentration of 100 mg/L. According to the literature [13], the synthesized biochar from oyster shells indicated the most Methylene Blue adsorption when the adsorbate concentration was upgraded from 25 mg/L to 50 mg/L. Based on the results of such studies, the percentage of removal and the amount of adsorption were 83% and 8.13 mg/g, respectively [13].

3.5. Effect of contact time

Figure 4d illustrates the function of synthesized Fe_3O_4/Char for Methylene Blue adsorption by varying contact times. The increasing trend of Methylene Blue adsorption was detected from 22.63% to 74.7%, while the contact time increased to 120 min. The most adsorption of Methylene Blue (53%) occurred in the initial 60 min when the more active sites were available for the adsorbate molecules [45]. In this context, Suhaimi, et al. [14] examined the adsorption rate of Methylene Blue by bamboo-based char, considering the contact time of 0-120 min. The highest adsorption rate, equal to 99%, was obtained at a contact time of 40 min. Another literature [24] evaluated the potential of char, derived from sludge pyrolysis, for Methylene Blue adsorption in a time duration of 60 min, of which almost 99% of Methylene Blue was adsorbed in 30 min.

3.6. Isotherm modeling

The Langmuir, Freundlich, Redlich-Peterson, and Temkin isotherm adsorption models were performed, as depicted in Figure 5. The constant values and determination coefficient (R^2) are indicated in Table 1, which were calculated by fitting experimental data with the isotherm models. The results demonstrated that the equilibrium adsorption data were better fitted with the Redlich-Peterson model (R^2= 0.9854). The Redlich-Peterson is a three-parameter-based isotherm model, which describes the formation of the monolayer with multisite interaction at the same time. Moreover, this model was applied to study homogeneous and heterogeneous adsorption systems [46]. While the R^2 values of Redlich-Peterson and Langmuir (R^2= 0.9818) were similar to each other, no single model can explain the adsorption mechanism, and the single-layer and multi-layer adsorption co-exist in this process. Furthermore, physisorption via weak electrostatic forces alongside chemisorption took place on the surface of the Fe_3O_4/Char [31]. However, regarding the γ value equal to 0.766, physisorption slightly dominated the chemisorption process [47]. On the other hand, the maximum adsorption capacity (q_m) in the Langmuir isotherm was relatively close to the experimental value, which determined the homogeneity of Fe_3O_4/Char and equal activation energy of each Methylene Blue molecule [48]. In this regard, To, et al. [49] demonstrated that the removal of pharmaceutical carbamazepine from water by waste biomass char followed the Redlich-Peterson isotherm, which confirmed that the adsorption was not obtained by a single identical reaction. Similar results were also achieved by Tang and Zaini [50], reporting the best fit with the Redlich-Peterson isotherm and Langmuir adsorption. In terms of the Freundlich isotherm model, the magnitude of the coefficient *n* denotes the favorability of the adsorption process. Therefore, the *n* value of 2.33 corresponded to a strong adsorbate–adsorbent bonding [51]. A higher amount of K_F also proved the strong bonding of Methylene Blue molecules on Fe_3O_4/Char. Notably, the Freundlich isotherm model displayed the multilayer coverage and the heterogeneous nature of the Fe_3O_4/Char [38]. However, the comparison of R^2 values is the basis for the application of the isotherm equation, which in this case, the Langmuir isotherm model was highly suited compared with the Freundlich isotherm model. The R^2 of Temkin isotherm (R^2= 0.9559) was lower than other models. The plotting ln C_e versus q_e determined the constants b_T and A_T, as shown in Table 1. The b_T value was calculated as 132.23 J/mol, lower than 1 kcal/mol, which depicted the physical adsorption occurrence [52]. The positive value of b_T also suggested that the adsorption of Methylene Blue onto the Fe_3O_4/Char was exothermic [51].

Table 1. Isotherm parameters and determination coefficient (R^2) of equilibrium isotherm models for Methylene Blue adsorption onto magnetic char (Fe_3O_4/Char) particles.

Isotherm	Parameters	Value
Langmuir	q_m (mg/g)	91.74
	b (L/mg)	0.040
	R^2	0.9818
Freundlich	K_F ($mg^{1-n}\ g^{-1}\ L^{-n}$)	10.53
	1/n	0.429
	R^2	0.9780
Redlich-Peterson	A_R (L/g)	6.754
	B_R $(L/mg)^{\beta}$	0.2382
	γ	0.766
	R^2	0.9854
Temkin	b_T (J/mol)	132.23
	A_T (L/g)	0.486
	R^2	0.9559

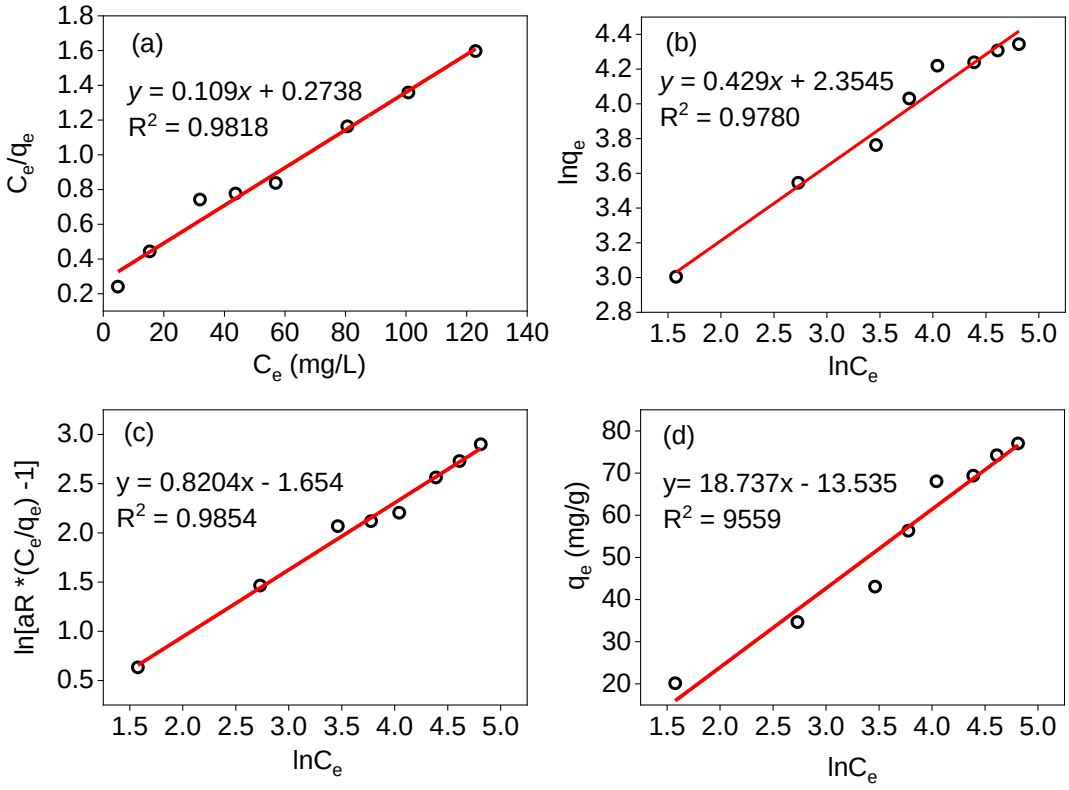

Fig. 5. Langmuir (a), Freundlich (b), Redlich-Peterson (c), and Temkin (d) isotherm models for Methylene Blue adsorption.

3.7. Kinetics modeling

The pseudo-first-order, pseudo-second-order, and Elovich kinetic models were applied to estimate the mechanism of the Methylene Blue adsorption process and determine the parameters that influence the reaction rate. As depicted in Figure 6 and Table 2, the Elovich kinetic model with an R^2 of 0.9397 can better explain the trend of experimental data rather than the Pseudo-first-order model (R^2= 0.8701) and Pseudo-second-order (R^2= 0.7983) models. The Elovich kinetic model showed that the active sites on the Fe_3O_4/Char were heterogeneous and demonstrated a range of activation energy throughout the adsorption process [53]. Moreover, this model indicated the chemical adsorption of Methylene Blue on the Fe_3O_4/Char with a β value of 0.027 g/mg. It should be mentioned that the β value attributes to the level of surface exposure and the activation energy of chemisorption [54]. On the other hand, the higher R^2 of the pseudo-first-order kinetic (0.8701) compared to the pseudo-second-order kinetic implied that Methylene Blue adsorption was more physical [55,56]. The results were compatible with Amin, et al. [57]; they utilized biochar to remove Methylene Blue dye and revealed the best fit of experimental data by Elovich (R^2 = 0.94) and pseudo-second-order (R^2 = 0.950) kinetic models. They reported the increased trend of initial adsorption rate constant (α) with increasing initial dye concentration [57]. Another literature [58], indicated the superiority of the Elovich kinetic (R^2 > 0.8742) to represent the Methylene Blue adsorption onto babassu coconut mesocarp biochar. They declared that the β value was higher at a lower initial dye concentration, which showed the favorable Methylene Blue capacity at a concentration of 150 mg/L [58].

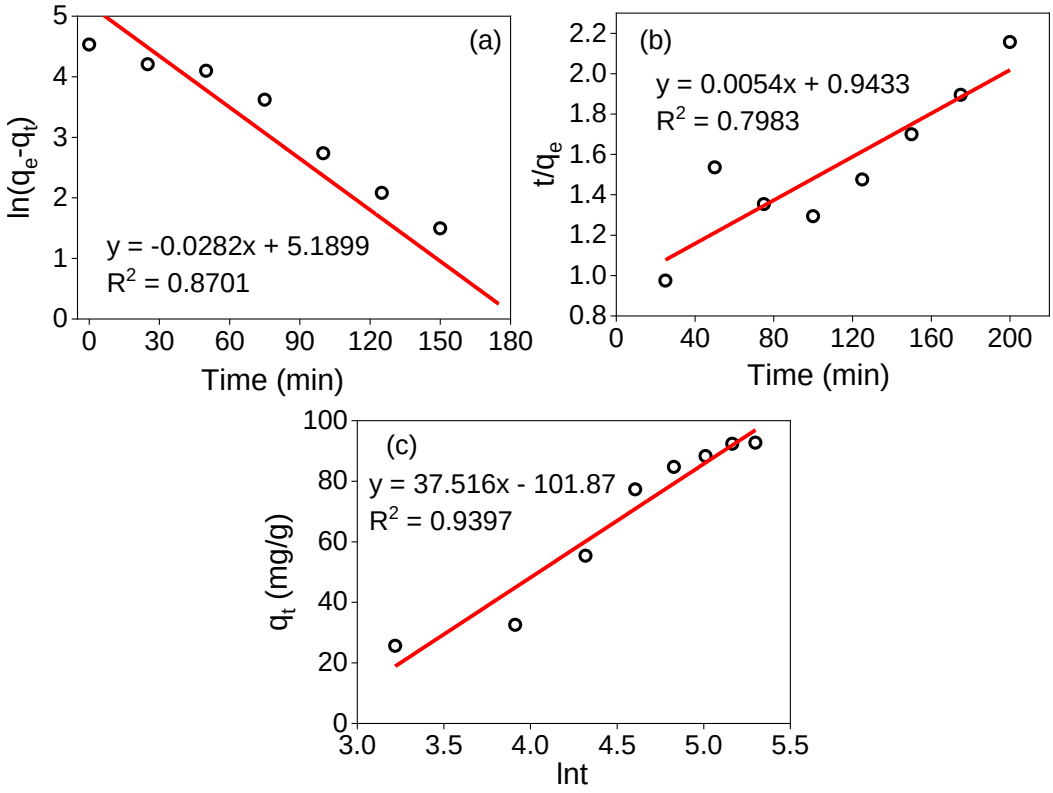

Fig. 6. Comparison of experimental and predicted pseudo-first-order (a), pseudo-second-order (b), and Elovich (c) kinetic models for the adsorption of Methylene Blue by magnetic char (Fe_3O_4/C) particles.

Table 2. Pseudo-first, pseudo-second-order, and Elovich kinetic model constants and determination coefficients (R^2) for the adsorption of Methylene Blue by magnetic char (Fe_3O_4/Char) particles

Kinetic model	Parameters	Value
Pseudo-first-order	q_{e1} (mg/g)	179.45
	k_1 (min^{-1})	0.0282
	R^2	0.8701
Pseudo-second-order	q_{e2} (mg/g)	185.19
	k_2 (g mg^{-1} min^{-1})	0.000031
	R^2	0.7983
Elovich	α (mg g^{-1} min^{-1})	2.483
	β (g/mg)	0.027
	R^2	0.9397

4. Conclusions

For the first time, a magnetic char (Fe_3O_4/Char) was synthesized from the oily sludge of a petrochemical refinery to appraise its capability for the adsorption of Methylene Blue. Various practical parameters, including pH, contact time, dye concentration, and adsorbent dosage, were considered to optimize the experiment. The highest Methylene Blue removal was achieved at a pH of 3, contact time of 120 min, Methylene Blue concentration of 100 mg/L, and an adsorbent dose of 100 mg. The maximum adsorption was 84%, accompanied by an adsorption capacity of 88.71 mg/g. The experimental data were fitted with the Redlich-Peterson isotherm model with an R^2 of 0.9854, indicating the physisorption and chemisorption of Methylene Blue on the surface of the Fe_3O_4/Char. The Langmuir and Freundlich isotherm models also represented the empirical data well, supporting monolayer adsorption and the surface heterogeneity onto the Fe_3O_4/Char. Furthermore, the experimental results showed that the adsorption process was well described by the Elovich kinetic model (R^2= 0.9397), which indicated the chemical adsorption. Regarding the considerable capacity of the oily sludge-based char for Methylene Blue adsorption and its porous structure, it can be a cost-effective and eco-friendly adsorbent for dye removal.

Acknowledgment

The authors wish to thank the Gorgan University of Agricultural Sciences and Natural Resources and Tarbiat Modares University, Iran.

References

[1] Xue, H., Wang, X., Xu, Q., Dhaouadi, F., Sellaoui, L., Seliem, M.K., Lamine, A.B., Belmabrouk, H., Bajahzar, A., Bonilla-Petriciolet, A. (2022). Adsorption of methylene blue from aqueous solution on activated carbons and composite prepared from an agricultural waste biomass: A comparative study by experimental and advanced modeling analysis. *Chemical engineering journal, 430*, 132801.

[2] Zahoor, M., Wahab, M., Salman, S.M., Sohail, A., Ali, E.A., Ullah, R. (2022). Removal of doxycycline from water using Dalbergia sissoo waste biomass based activated carbon and magnetic oxide/activated bioinorganic nanocomposite in batch adsorption and adsorption/membrane hybrid processes. *Bioinorganic chemistry and applications*, 2694487.

[3] Singh, V., Srivastava, V.C. (2022). Hazardous maize processing industrial sludge: Thermo-kinetic assessment and sulfur recovery by evaporation-condensation technique. *Journal of hazardous materials, 424*, 127477.

[4] Freeman, H.S., Dos Santos, T.C., Chen, Y., Vendemiatti, J.A., de Oliveira, A.C., Vacchi, F.I., Vinueza, N.R., Umbuzeiro, G.A. (2022). Molecular characterization and ecotoxicological evaluation of the natural dye madder and its chlorinated products. *Environmental science and pollution research, 29*(16), 24261-24268.

[5] Zhai, S., Li, M., Wang, D., Zhang, L., Yang, Y., Fu, S. (2019). In situ loading metal oxide particles on bio-chars: Reusable materials for efficient removal of methylene blue from wastewater. *Journal of cleaner production, 220*, 460-474.

[6] Moyo, S., Makhanya, B.P., Zwane, P.E. (2022). Use of bacterial isolates in the treatment of textile dye wastewater: A review. *Heliyon*, e09632.

[7] Hevira, L., Ighalo, J.O., Aziz, H., Zein, R. (2021). Terminalia catappa shell as low-cost biosorbent for the removal of methylene blue from aqueous solutions. *Journal of industrial and engineering chemistry, 97*, 188-199.

[8] Jabar, J.M., Odusote, Y.A. (2020). Removal of cibacron blue 3G-A (CB) dye from aqueous solution using chemo-physically activated biochar from oil palm empty fruit bunch fiber. *Arabian journal of chemistry, 13*(5), 5417-5429.

[9] Dao, T.M., Le Luu, T. (2020). Synthesis of activated carbon from macadamia nutshells activated by H2SO4 and K_2CO_3 for methylene blue removal in water. *Bioresource technology reports, 12,* 100583.

[10] Jia, P., Tan, H., Liu, K., Gao, W. (2018). Removal of methylene blue from aqueous solution by bone char. *Applied sciences, 8*(10), 1903.

[11] Pinheiro, L.R.S., Gradíssimo, D.G., Xavier, L.P., Santos, A.V. (2022). Degradation of Azo Dyes: bacterial potential for bioremediation. *Sustainability, 14*(3), 1510.

[12] Viswanthan, S.P., Neelamury, S.P., Parakkuzhiyil, S., Njazhakunnathu, G.V., Sebastian, A., Padmakumar, B., Ambatt, T.P. (2020). Removal efficiency of methylene blue from aqueous medium using biochar derived from Phragmites karka, a highly invasive wetland weed. *Biomass conversion and biorefinery,* 1-17.

[13] Kaya, N., Yıldız, Z., Ceylan, S. (2018). Preparation and characterisation of biochar from hazelnut shell and its adsorption properties for methylene blue dye. *Politeknik dergisi, 21*(4), 765-776.

[14] Suhaimi, N., Kooh, M.R.R., Lim, C.M., Chou Chao, C.-T., Chou Chau, Y.-F., Mahadi, A.H., Chiang, H.-P., Haji Hassan, N.H., Thotagamuge, R. (2022). The Use of Gigantochloa Bamboo-Derived Biochar for the Removal of Methylene Blue from Aqueous Solution. *Adsorption science and technology*, 8245797.

[15] Chegini, G., Briens, C., Pjontek, D. (2022). Production and characterization of adsorbents from a hydrothermal char by pyrolysis, carbon dioxide and steam activation. *Biomass conversion and biorefinery*, 1-17.

[16] Wang, L., Jiang, J., Ma, J., Pang, S., Zhang, T. (2022). A review on advanced oxidation processes homogeneously initiated by copper (II). *Chemical engineering journal, 427*, 131721.

[17] Karaghool, H.A., Hashim, K., Kot, P., Muradov, M. (2022). Preliminary studies of methylene blue remotion from aqueous solutions by ocimum basilicum. *Environments, 9*(2), 17.

[18] Ulfa, M., Setiarini, I. (2022). Study The Effect of Zinc Oxide Supported on Gelatin Mesoporous Silica (GSBA-15) on Structural Character and Their Methylene Blue Photodegradation Performance. *Bulletin of chemical reaction engineering and catalysis, 17*(2), 363-374.

[19] Su, H., Guo, X., Zhang, X., Zhang, Q., Huang, D., Lin, L., Qiang, X. (2022). Ultrafine biosorbent from waste oyster shell: A comparative study of Congo red and Methylene blue adsorption. *Bioresource technology reports, 19*, 101124.

[20] Dunnett, A.J., Gowland, D., Isborn, C.M., Chin, A.W., Zuehlsdorff, T.J. (2021). Influence of non-adiabatic effects on linear absorption spectra in the condensed phase: Methylene blue. *The journal of chemical physics, 155*(14), 144112.

[21] Han, F., Zhang, M., Liu, Z., Han, Y., Li, Q., Zhou, W. (2022). Enhancing robustness of halophilic aerobic granule sludge by granular activated carbon at decreasing temperature. *Chemosphere, 292*, 133507.

[22] Priya, A.K., Gokulan, R., Vijayakumar, A., Praveen, S. 2020. Biodecolorization of remazol dyes using biochar derived from *Ulva reticulata*: isotherm, kinetics, desorption, and thermodynamic studies. *Desalination and water treatment*, 200, 286–295.

[23] Pandey, D., Daverey, A., Dutta, K., Yata, V.K., Arunachalam, K. (2022). Valorization of waste pine needle biomass into biosorbents for the removal of methylene blue dye from water: Kinetics, equilibrium and thermodynamics study. *Environmental technology and innovation, 25*, 102200.

[24] Hu, M., Deng, W., Hu, M., Chen, G., Zhou, P., Zhou, Y., Su, Y. (2021). Preparation of binder-less activated char briquettes from pyrolysis of sewage sludge for liquid-phase adsorption of methylene blue. *Journal of environmental management, 299*, 113601.

[25] Ghosh, I., Kar, S., Chatterjee, T., Bar, N., Das, S.K. (2021). Removal of methylene blue from aqueous solution using Lathyrus sativus husk: adsorption study, MPR and ANN modelling. *Process safety and environmental protection, 149*, 345-361.

[26] Ighalo, J.O., Arowoyele, L.T., Ogunniyi, S., Adeyanju, C.A., Oladipo-Emmanuel, F.M., Belgore, O.R., Omisore, M.O., Adeniyi, A.G. (2021). Utilisation of biomass and hybrid biochar from elephant grass and low density polyethylene for the competitive adsorption of Pb (II), Cu (II), Fe (II) and Zn (II) from aqueous media. *Recent innovations in chemical engineering (Formerly recent patents on chemical engineering), 14*(2), 148-159.

[27] Sachdev, D., Shrivastava, H., Sharma, S., Srivastava, S., Tadepalli, S., Bhullar, N.K., Sahu, O.P. (2022). Potential for hydrothermally separated groundnut shell fibers for removal of methylene blue dye. *Materials today: proceedings, 48*, 1559-1568.

[28] KÜÇÜK, İ., Yunus, Ö., BAŞAR, C. (2021). The activated carbon from walnut shell using CO_2 and methylene blue removal. *Dicle Üniversitesi Mühendislik Fakültesi Mühendislik Dergisi, 12*(2), 297-308.

[29] Shelke, H.D., Machale, A.R., Survase, A.A., Pathan, H.M., Lokhande, C.D., Lokhande, A.C., Shaikh, S.F., Palaniswami, M. (2022). Multifunctional Cu_2SnS_3 Nanoparticles with Enhanced Photocatalytic Dye Degradation and Antibacterial Activity. *Materials, 15*(9), 3126.

[30] Sarojini, G., Babu, S.V., Rajamohan, N., Rajasimman, M., Pugazhendhi, A. (2022). Application of a polymer-magnetic-algae based nano-composite for the removal of methylene blue–characterization, parametric and kinetic studies. *Environmental pollution, 292*, 118376.

[31] Shahnaz, T., Bedadeep, D., Narayanasamy, S. (2022). Investigation of the adsorptive removal of methylene blue using modified nanocellulose. *International journal of biological macromolecules, 200,* 162-171.

[32] Feizi, F., Sarmah, A.K., Rangsivek, R., Gobindlal, K. (2022). Adsorptive removal of

propranolol under fixed-bed column using magnetic tyre char: Effects of wastewater effluent organic matter and ball milling. *Environmental pollution, 305*, 119283.

[33] Li, J., Han, L., Zhang, T., Qu, C., Yu, T., Yang, B. (2022). Removal of Methylene Blue by Metal Oxides Supported by Oily Sludge Pyrolysis Residues. *Applied sciences, 12*(9), 4725.

[34] Jabar, J.M., Odusote, Y.A., Ayinde, Y.T., Yılmaz, M. (2022). African almond (Terminalia catappa L) leaves biochar prepared through pyrolysis using H3PO4 as chemical activator for sequestration of methylene blue dye. *Results in engineering, 14,* 100385.

[35] Liu, Y., Jiang, Z., Fu, J., Ao, W., Siyal, A.A., Zhou, C., Liu, C., Dai, J., Yu, M., Zhang, Y. (2022). Iron-biochar production from oily sludge pyrolysis and its application for organic dyes removal. *Chemosphere, 301*, 134803.

[36] Zhang, J., Cai, D., Zhang, G., Cai, C., Zhang, C., Qiu, G., Zheng, K., Wu, Z. (2013). Adsorption of methylene blue from aqueous solution onto multiporous palygorskite modified by ion beam bombardment: Effect of contact time, temperature, pH and ionic strength. *Applied clay science, 83*, 137-143.

[37] Huang, W., Pan, S., Yu, Q., Liu, X., Liu, Y., Liu, R. (2019). Adsorption performance of methyl blue onto magnetic Ni (1– x– y) CuyZnxFe2O4 nanoparticles prepared by a novel alcohol-assisted combustion method. *Journal of Inorganic and organometallic polymers and materials*, 29(5), 1755-1766.

[38] Peer, F.E., Bahramifar, N., Younesi, H. (2018). Removal of Cd (II), Pb (II) and Cu (II) ions from aqueous solution by polyamidoamine dendrimer grafted magnetic graphene oxide nanosheets. *Journal of the Taiwan Institute of Chemical Engineers*, 87, 225-240.

[39] Saffari, M., Moazallahi, M. (2022). Evaluation of slow-pyrolysis process effect on adsorption characteristics of cow bone for Ni ion removal from Ni-contaminated aqueous solutions. *Pollution*, *8*(3), 1076-1087.

[40] Das, S., Goud, V.V. (2020). Characterization of a low-cost adsorbent derived from agro-waste for ranitidine removal. *Materials science for energy technologies, 3*, 879-888.

[41] Padmapriya, M., Ramesh, S., Biju, V. (2022). Synthesis of seawater based geopolymer: characterization and adsorption capacity of methylene blue from wastewater. *Materials Today: Proceedings*, 51, 1770-1776.

[42] Villabona-Ortíz, Á., Figueroa-Lopez, K.J., Ortega-Toro, R. (2022). Kinetics and Adsorption Equilibrium in the Removal of Azo-Anionic Dyes by Modified Cellulose. *Sustainability*, 14(6), 3640.

[43] Kooh, M.R.R., Thotagamuge, R., Chau, Y.-F.C., Mahadi, A.H., Lim, C.M. (2022). Machine learning approaches to predict adsorption capacity of Azolla pinnata in the removal of methylene blue. *Journal of the Taiwan Institute of Chemical Engineers*, 132, 104134.

[44] Jia, S., Han, H., Hou, B., Zhuang, H., Fang, F., Zhao, Q. (2014). Treatment of coal gasification wastewater by membrane bioreactor hybrid powdered activated carbon (MBR–PAC) system. *Chemosphere*, 117, 753-759.

[45] Gao, Y., Hao, B., Xue, N., Wang, Y., Xiao, H., Huang, X., Shi, B. (2022). Steam activation tuned porous structure and surface wetting behaviors of mesoporous biochars for corrosive oily wastewater treatments. *Journal of Chemical Technology & Biotechnology*, 2179-2185.

[46] Elmorsi, R.R., Abou-El-Sherbini, K.S., Shehab El-Dein, W.A., Lotfy, H.R. (2022). Activated eco-waste of Posidonia oceanica rhizome as a potential adsorbent of methylene blue from saline water. *Biomass Conversion and Biorefinery*, 1-14.

[47] Tang, X., Ran, G., Li, J., Zhang, Z., Xiang, C. (2021). Extremely efficient and rapidly adsorb methylene blue using porous adsorbent prepared from waste paper: Kinetics and equilibrium studies. *Journal of hazardous materials*, 402, 123579.

[48] Bounaas, M., Bouguettoucha, A., Chebli, D., Gatica, J.M., Vidal, H. (2021). Role of the wild carob as biosorbent and as precursor of a new high-surface-area activated carbon for the adsorption of methylene blue. *Arabian journal for science and engineering, 46*(1), 325-341.

[49] To, M.-H., Hadi, P., Hui, C.-W., Lin, C.S.K., Tareq, A.-A., Saleem, J., Parthasarathy, P., McKay, G. (2019). Waste biomass gasification

char derived activated carbon for pharmaceutical carbamazepine removal from water. *Resources environment and information engineering*, *1*(1), 36-44.

[50] Tang, S.H., Zaini, M.A.A. (2019). Isotherm studies of malachite green removal by yarn processing sludge-based activated carbon. *Chemistry-didactics-ecology-metrology*, *24*.

[51] Shikuku, V.O., Mishra, T. (2021). Adsorption isotherm modeling for methylene blue removal onto magnetic kaolinite clay: a comparison of two-parameter isotherms. *Applied water science*, *11*(6), 1-9.

[52] Ettish, M.N., El-Sayyad, G.S., Elsayed, M.A., Abuzalat, O. (2021). Preparation and characterization of new adsorbent from Cinnamon waste by physical activation for removal of Chlorpyrifos. *Environmental challenges*, *5*, 100208.

[53] Dermawan, D., Febrianti, A.N., Setyawati, E.E.P., Pham, M.-T., Jiang, J.-J., You, S.-J., Wang, Y.-F. (2022). The potential of transforming rice straw (Oryza sativa) and golden shower (Cassia fistula) seed waste into high-efficiency biochar by atmospheric pressure microwave plasma. *Industrial Crops and Products*, 185, 115122.

[54] Xiao, Y., Tian, L., Liu, X. (2022). Kinetic mechanism on elemental mercury adsorption by brominated petroleum coke in simulated flue gas. *RSC Advances*, 12(26), 16386-16395.

[55] Chandarana, H., Kumar, P.S., Seenuvasan, M., Kumar, M.A. (2021). Kinetics, equilibrium and thermodynamic investigations of methylene blue dye removal using Casuarina equisetifolia pines. *Chemosphere*, 285, 131480.

[56] Fakhar, N., Khan, S.A., Khan, T.A., Siddiqi, W.A. (2022). Efficiency of iron modified Pyrus pyrifolia peels biochar as a novel adsorbent for methylene blue dye abatement from aqueous phase: equilibrium and kinetic studies. *International Journal of Phytoremediation*, 1-11.

[57] Amin, M.T., Alazba, A.A., Shafiq, M. (2021). Successful application of eucalyptus camdulensis biochar in the batch adsorption of crystal violet and methylene blue dyes from aqueous solution. *Sustainability*, 13(7), 3600.

[58] Kasemodel, M.C., Romão, E.L., Papa, T.B.R. (2022). Adsorption of methylene blue on babassu coconut (Orbignya speciosa) Mesocarp commercial biochar, *Research square*, 1-21.